New Journal of Physics
The open-access journal for physics

Approach to ordered structure of the beam at S-LSR

A Noda[1], **M Ikegami and T Shirai**
Institute for Chemical Research, Kyoto University, Gokasho,
Uj-cityi, Kyoto 611-0011, Japan
E-mail: noda@kyticr.kuicr.kyoto-u.ac.jp

New Journal of Physics **8** (2006) 288
Received 28 June 2006
Published 28 November 2006
Online at http://www.njp.org/
doi:10.1088/1367-2630/8/11/288

Abstract. An approach with S-LSR at ICR, Kyoto University to attain an ordered structure for a circulating beam in a storage ring with a speed that is not negligible compared with the light velocity is described. An experimental approach for one-dimensional (1D) ordering of a 7 MeV proton beam with the use of electron beam cooling is given first and then experimental plans to realize crystalline structures of $^{24}Mg^{+}$ ions with a kinetic energy of 35 keV by applying laser cooling are described together with computer-simulation results by a molecular dynamics (MD) code.

[1] Author to whom any correspondence should be addressed.

PII: S1367-2630(06)27612-2

Contents

1. Introduction

The beams in an accelerator are, in general, in the gas phase and their temperatures are usually very high. Stimulated by a first report on an indication of realizing one-dimensional (1D) ordering from NAPM at BINP (Budker Institute of Nuclear Physics) [1], various experimental approaches for ordered states have been performed and 1D ordering of heavy ions with higher charge than C^{6+} has been reported from ESR and SIS at GSI [2] and CRYRING at Manne Siegbahn Laboratory in Stockholm [3]. In these cases, their temperature is not very low (around several hundred kelvin in transverse direction), and the line density is rather low. The reason is that the efficiency of electron cooling becomes lower as the temperature of the ion beam decreases, and the heating rate by intra-beam scattering (IBS) increases as the line density of the beam increases [4].

In order to generate a crystalline beam of higher line density, we must develop a strong 3D cooling force that can exceed the heating rate by IBS. For this purpose, laser cooling of the ion beam is inevitable. The laser cooling of stored ion beams, however, is effective only for the longitudinal degree of freedom. As a method to overcome such a problem, 3D laser cooling by a resonant coupling method has been proposed [5, 6]. With the use of the resonant coupling method, the creation of 1D and 2D crystalline beams is expected [7, 8]. The formation of a 3D ordered state by using laser cooling at the RF-Quadrupole Ring Trap, PALLAS has been reported from Munich [9], which, however, is known to be broken for energies higher than 1 eV.

The laser cooling force arranges all particles to have the same linear velocity. On the other hand, all particles are required to have the same angular velocity at the bending sections in order to keep the ordered structures having a horizontal extent in the ring, because the betatron oscillation is frozen when beam cooling proceeds well. When the centre of mass of the crystalline beam has a certain amount of velocity, a bending section composed of a pure magnetic field cannot realize the same angular velocity for all ions set to be the same energy at the straight section, as illustrated in figure 1, and the difference in the angular velocity breaks the crystalline structure.

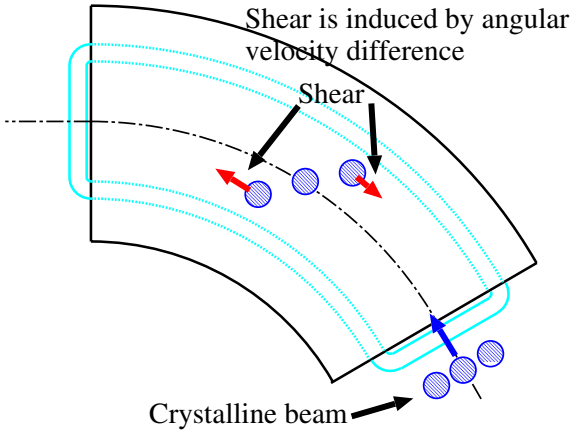

Figure 1. Illustration of shear. If the crystalline beam is bent by a pure magnetic field, the outer particle locates behind the inner particle. Note that the betatron motion freezes in the crystalline state.

Table 1. Main parameters of S-LSR.

Ion species (energy)	H^+(7 MeV) $^{12}C^{6+}$(2 MeV/u) $^{24}Mg^+$(35 keV)
Cooling methods	Electron beam cooling, laser cooling
Circumference	22.557 m
Average radius	3.59 m
Length of straight section	2.66 m
Number of periods	6
Betatron tune (ν_x, ν_y)	
Electron cooling	(1.64, 1.21)
Laser cooling	(2.07, 1.07); (2.07, 2.07); (1.44, 1.44)
Bending magnet	(H-type)
Maximum field	0.95 T
Curvature radius	1.05 m
Gap height	70 mm
Pole end cut	Rogowskii cut + field clamp
Deflection angle	60°
Weight	4.5 tons
Quadrupole magnet	
Core length	0.20 m
Bore radius	70 mm

Such an effect is called 'shear' [10]. In order to generate a 3D crystalline state of a fast ion beam in storage rings, we have to overcome this 'shear'. For this purpose, we propose two possibilities. They are shown in sections 3 and 4.

The scope of the present paper is to show a way to realize multidimensional ordered states at S-LSR, while managing any difficulties so far known, based on previous efforts all over the world, as mentioned above. S-LSR is a storage and cooler ring, completed in the autumn of 2005 at Institute for Chemical Research, Kyoto University. Its main parameters are listed in table 1 and its layout and overall view are shown in figures 2 and 3, respectively [11].

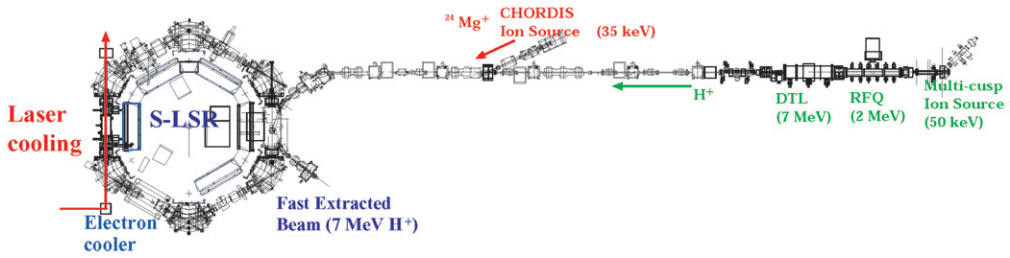

Figure 2. Layout of the ion storage cooler ring, S-LSR.

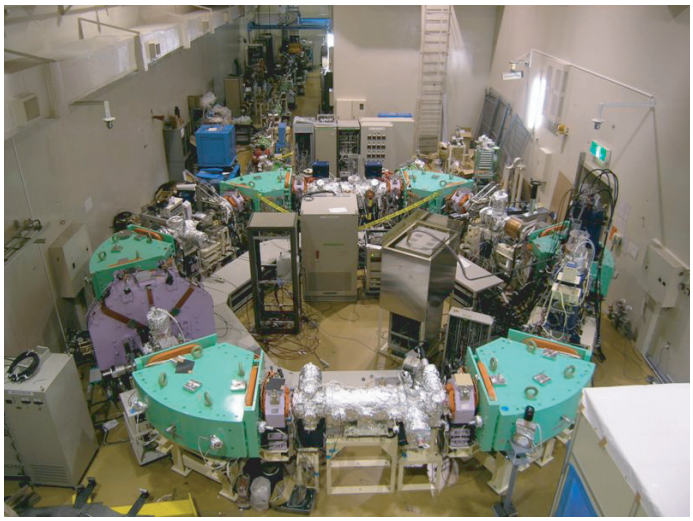

Figure 3. An overall view of S-LSR.

First, the recent experimental approach to the lowest temperature limit by applying electron beam cooling for 7 MeV protons is given. Then possible experiments at S-LSR to realize various crystalline structures with the application of laser cooling for 35 keV $^{24}Mg^{+}$ ions are presented from a theoretical point of view along with the results of a molecular dynamics (MD) simulation.

2. Experimental approach to an ordered structure by electron cooling

2.1. 1D ordering of heavy ions by electron cooling

The electron cooler is a powerful tool to reduce the temperature of the ion beam. But usually the ion temperature is determined by the IBS, not by the electron temperature. Only at very low intensity, can the ion beam temperature be close to the electron one because the IBS becomes weak. The first clear evidence of the 1D ordering of the ion beam was found at ESR in GSI [2]. The stored ion was $^{197}Au^{79+}$ at the energy of 360 MeV/u. When the number of stored ions was reduced to less than a few thousand, the momentum spread of the beam dropped abruptly below 10^{-6}. This is interpreted as phenomena where each particle is reflected by the Coulomb collisions with neighbours and they do not overtake each other in the longitudinal direction [12]–[15]. They were found for C^{6+}, Ar^{18+}, Ni^{28+}, Kr^{36+}, Au^{79+} and U^{92+} [16]. In CRYRING, similar phenomena

Table 2. Comparison of the parameters of NAPM, COSY and S-LSR.

Energy	NAPM	COSY	S-LSR
Circumference	47.25 m	183.5 m	22.557 m
Proton energy	65 MeV	45.6 MeV	7 MeV
Betatron tune (ν_x, ν_y)	(1.34, 1.24)	(3.62, 3.68)	(1.64, 1.21)
Cooler length	1.0 m	1.4 m	0.45 m
Magnetic field	1 kG	0.8 kG	0.5 kG
Beam current	1 A	50 mA–1 A	25 mA–0.3 A
Beam radius	0.5 cm	1.27 cm	2.5 cm

were observed for Ni^{17+}, Kr^{33+}, Xe^{36+} and Pb^{55+} [3]. The transition has not been reported for ions with lower charge ($q < 6$). One reason is that low charge number results in weak Coulomb interaction between ions. The other reason is that the momentum spread of the heavier ions reaches the smaller value when the ion temperature is close to the electron temperature, because the ion temperature $T_{i\|}$ is given by the following formula,

$$k_B T_{i\|} = m_i \nu_0^2 \left(\frac{\delta p}{p}\right)^2, \tag{1}$$

where m_i is the ion mass and ν_0 is the ion velocity.

A search of the 1D ordering of ions with low charge, especially the proton beam, is important for the verification of the ordering theory under the weakest limit of the Coulomb interaction. The 1D ordering experiments for protons have been reported in two rings prior to our S-LSR. They are shown in the table 2 together with our case. In NAPM, the dependence of the momentum spread on the proton number showed the very specific character [1]. When the number of the proton was reduced less than 10^7, the momentum spread stopped decreasing at the very small value of 1×10^{-6} and remained constant. In COSY, similar phenomena were observed. The momentum spread became almost constant at a proton number of less than 10^6 [17]. But the sudden drop of the momentum spread was not observed and it seems that the proton beam did not reach the ordered state. NAPM has already stopped operation and S-LSR has an advantage of the larger ratio of the cooler length to the circumference compared with COSY.

2.2. Electron temperature in the S-LSR electron cooler

The temperature of the cooled ions is determined by the electron temperature if the IBS is negligible. The electron beam has a flattened distribution in velocity space. The longitudinal electron temperature ($T_{e\|}$) is greatly reduced by static acceleration. On the other hand, the transverse temperature is reduced only by the magnetic expansion factor (α). They are given by [18]

$$k_B T_{e\|} = \frac{(k_B T_{cath})^2}{2eU} + C\frac{e^2 n_e^{1/3}}{4\pi\varepsilon_0}, \qquad k_B T_{e\perp} = \frac{k_B T_{cath}}{\alpha}, \tag{2}$$

where n_e is the electron density and U is the static acceleration voltage. C is a constant factor of 1.9, which depends on the electron gun structure. T_{cath} is the cathode temperature of the electron gun, which is 900°C in the case of the S-LSR cooler. Table 3 gives the typical parameters of the

Table 3. Parameters of the electron beam cooler.

Energy	3.8 keV
Electron beam current (typ.)	50 mA
Beam diameter	50 mm
Beam density	4.4×10^{6} e^{-} cm^{-3}
Solenoid field in the central	500 Gauss
Expansion factor	3
Effective cooling length	440 mm

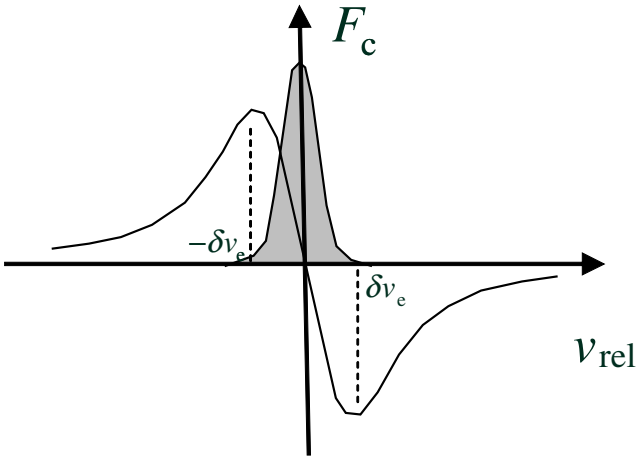

Figure 4. Schematic drawing of the electron cooling force and the cooled ion beam.

electron cooler in S-LSR [19]. The calculated longitudinal temperature is 46 μeV (0.5 K) and the transverse one is 34 meV (390 K) under this condition. The longitudinal temperature is also affected by the external heating source, such as the power supply ripple and the inhomogeneous magnetic field in the cooling section. Cooling force measurements were made to estimate the electron temperature. They were measured by an induction accelerator [20]. The ion beam was trapped at the equilibrium point of the electron cooling potential (see figure 4). The equilibrium point was shifted by the induction force and the cooling force was calculated from the induction voltage and the velocity shift. The measurement results are shown in figure 5. In a binary collision model of the electron cooling, the cooling force has a maximum value when the longitudinal electron velocity spread is almost equal to the relative velocity (δv_e). The maximum point is at a relative velocity of 3500 m s^{-1} in figure 5, which corresponds to the longitudinal electron temperature of 35 μeV (0.4 K). The difference from the calculated value with the use of equation (2) (46 μeV (0.5 K)) is considered to be explained by the uncertainty in estimation of T_{cath} and n_e and the analytical model of the electron cooling.

2.3. 1D ordering simulation of the proton beam at S-LSR

When each particle is reflected by Coulomb collisions with neighbours, the reflection probability is given by the Hamiltonian of the system [15]. It depends on the longitudinal and transverse temperatures of the ion beams. Figure 6 shows the calculated reflection probability lines of

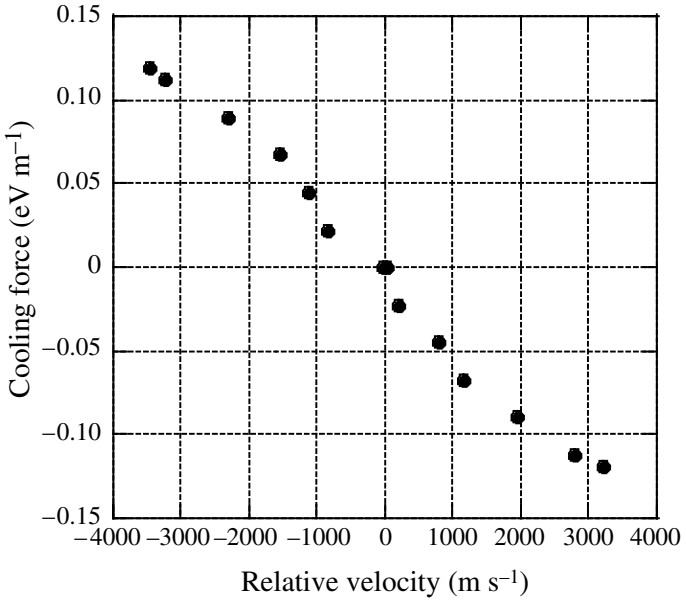

Figure 5. Measured cooling force using an induction accelerator. The electron current is 50 mA and the ion current is 0.1 μA.

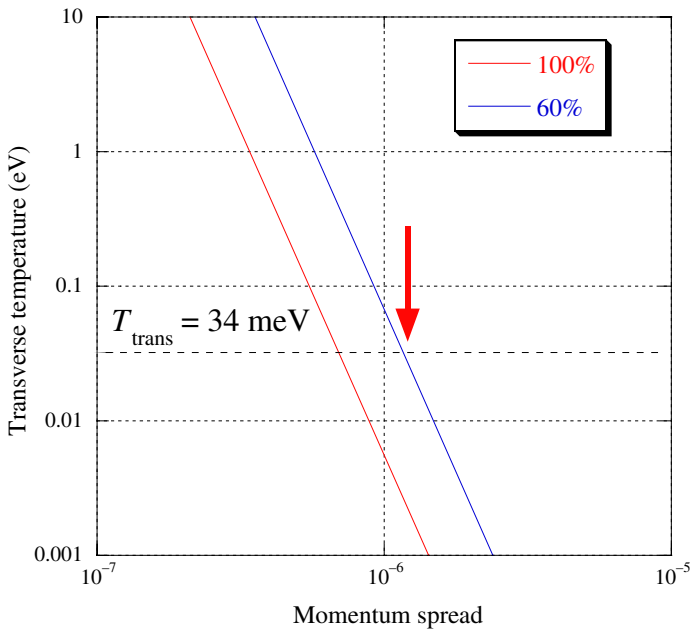

Figure 6. Calculated reflection probability of a 7 MeV proton; the red line shows 100% and the blue line shows 60%. The red arrow corresponds to the calculated minimum ion temperature.

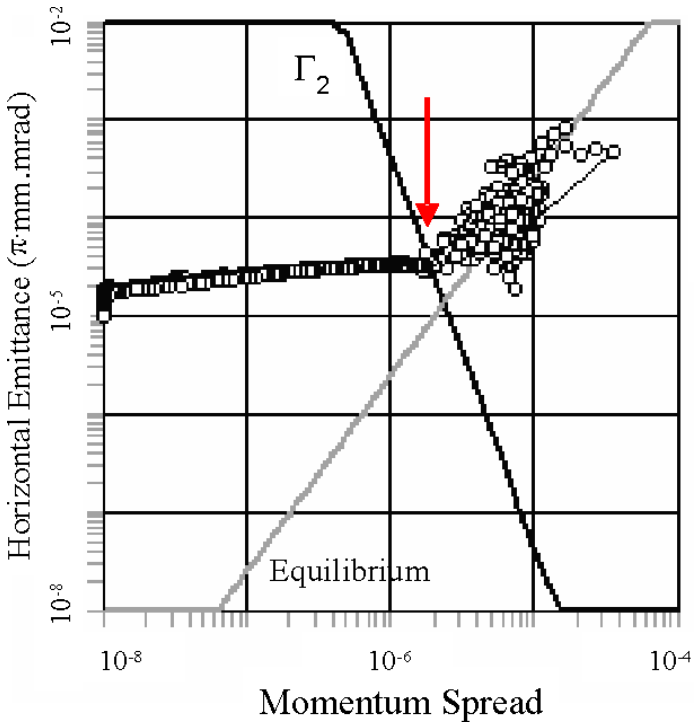

Figure 7. MD simulation results with a particle number of 3000. The transition to the ordered state is observed at a momentum spread of $\delta P/P = 2 \times 10^{-6}$.

100 and 60% for S-LSR. Most of the 1D ordering phenomena of the heavy ion beams are observed when the reflection probability is between 60 and 70%. The expected transition point to the 1D ordering is at a momentum spread of 1.2×10^{-6} when the ion transverse temperature is 34 meV, which is the electron temperature of the S-LSR cooler.

The MD simulation also predicts the 1D ordering of the proton beam at S-LSR. A simulation of particle dynamics was carried out with a realistic electron cooling force and parameters of the electron beam and the ring [21]. The program is BETACOOL, which is a particle tracking code in the storage ring, including the some kinds of cooling effects [22]. Figure 7 shows the MD simulation results with a particle number of about 3000. The Γ_2 line is a criterion of the ordering [14]. The transition to the ordered state can be observed at a momentum spread of $\delta \mathrm{P}/\mathrm{P} = 2 \times 10^{-6}$.

The two independent calculation methods expect 1D ordering of the proton beam at S-LSR when the momentum spread is around 1.2×10^{-6} to 2×10^{-6}. If the longitudinal ion temperature is the same as that of the electron of 35 μeV, the minimum ion momentum spread is given by equation (1). It is 2×10^{-6} and close to the threshold value.

2.4. 1D ordering experiments of the proton beam at S-LSR

In order to reduce the effect of IBS, we measured the momentum spread of 7 MeV proton beam, while reducing the particle number (N_p). The results are shown in figure 8 with three different electron currents of the cooler. The momentum spread was measured by a Schottky monitor [23] and the particle number was measured by a residual-gas monitor using a micro-channel plate

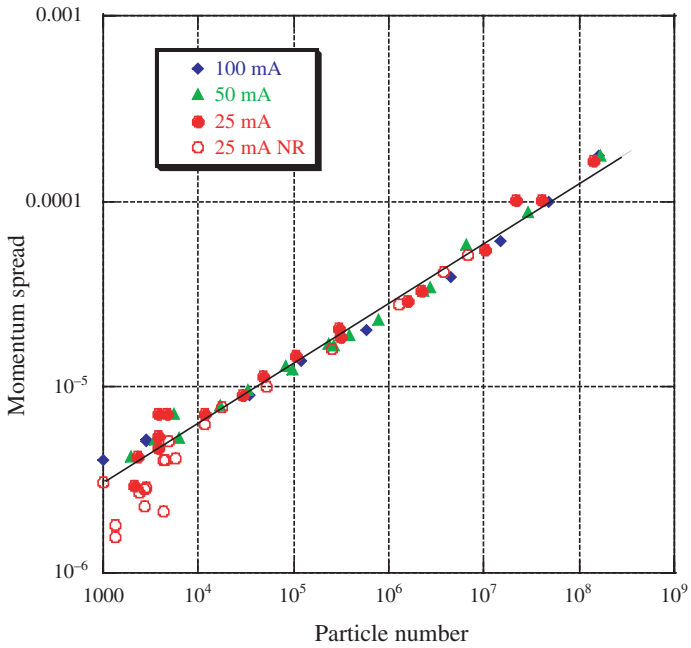

Figure 8. Dependence of the ion momentum spread on the particle number with three different electron currents.

(MCP) [24]. The measured data show very weak dependence on the electron current as shown in figure 8. For lower electron current, the space charge effect is expected to be small, which results in lower electron temperature. So we repeated the above measurement with the electron current of 25 mA after the efforts to reduce the noise level of the Schottky monitor, cooling the head amplifier to a temperature lower than −20°C and inserting line filter into the AC line (plotted by '○' and denoted as 25 mA NR). The solid line in figure 8 is a fitting to all the data above the particle number of 10^4 and the momentum spread is found to be proportional to $N_p^{0.31}$. In this recent measurement at the electron current of 25 mA with reduction of noise level, we have observed systematic reduction of fractional momentum spread for particle numbers lower than several thousands. Figure 9 shows the relation between the Schottky power and the particle number in the same measurements. Data points for the same conditions also deviate from the fitting line. A similar anomaly of the Schottky power has been reported at CRYRING for the 1D ordered states of heavy ions [3]. The above anomalies we have observed in the fractional momentum spread and the Schottky power might be an indication of 1D ordering of 7 MeV proton beam although they are relatively small compared with the cases of the heavy ions.

3. Approach to multidimensional crystalline beams by laser cooling

3.1. Necessary conditions to create crystalline beams

As discussed in section 2, it is difficult to create multidimensional crystalline beams by electron cooling due to the property of the cooling force and IBS. The limitation of electron cooling, which becomes weaker in the low-temperature region, can be overcome by applying 3D laser cooling with a resonant coupling method.

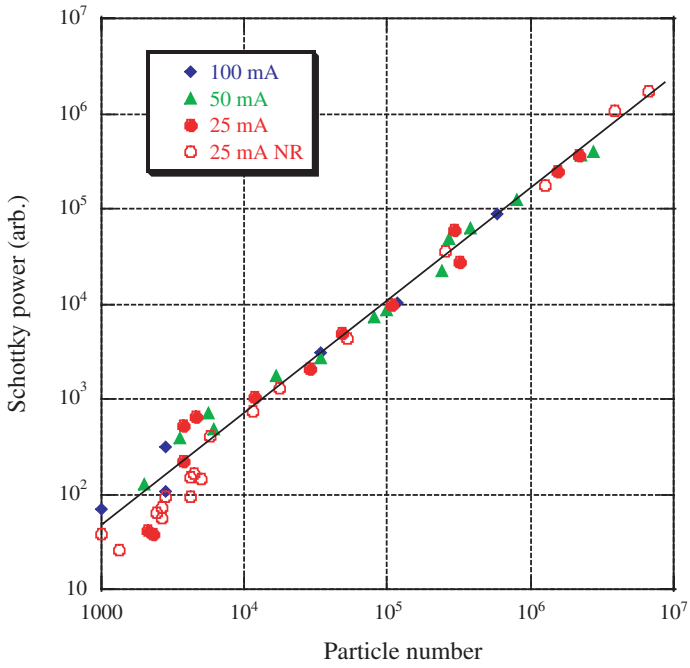

Figure 9. Schottky power as a function of the particle number. The experimental conditions are the same as those of figure 8.

The characteristics of multidimensional crystalline beams has been theoretically studied by using MD simulations assuming a time-independent uniform focusing force [25, 26]. In actual accelerators, the beam receives a discrete focusing force from quadrupole magnets. Furthermore, in a circular machine, the beam is bent by bending magnets. Under such conditions, it has been found that the storage ring must satisfy the so-called formation and maintenance conditions to create crystalline beams [10, 27],

$$\gamma < \gamma_t, \tag{3}$$

$$N_{SP} > 2\sqrt{\nu_x^2 + \nu_y^2}, \tag{4}$$

where γ is the Lorentz gamma of the beam, γ_t is the transition gamma, N_{SP} is the number of superperiods of the ring, and ν_x and ν_y are betatron tunes in the horizontal and vertical directions, respectively. The formation condition means that the lattice must be strongly focusing, which can operate below the transition energy. The maintenance condition is necessary to keep crystallized beams stably avoiding linear resonance between the phonon oscillation of crystals and the periodic external force of the ring [27].

When the line density of the beam is high, a stricter condition than equation (4) is required: in this case, coherent resonances which prevent the cooling occur at a certain temperature. Since the cooling of beams inevitably start from a high temperature state, the beams always cross such resonances. However, we can avoid the occurrence of dangerous linear resonances at all temperature regions, when the following condition is satisfied [28],

$$N_{SP} > 4 \cdot \nu_{x(y)}. \tag{5}$$

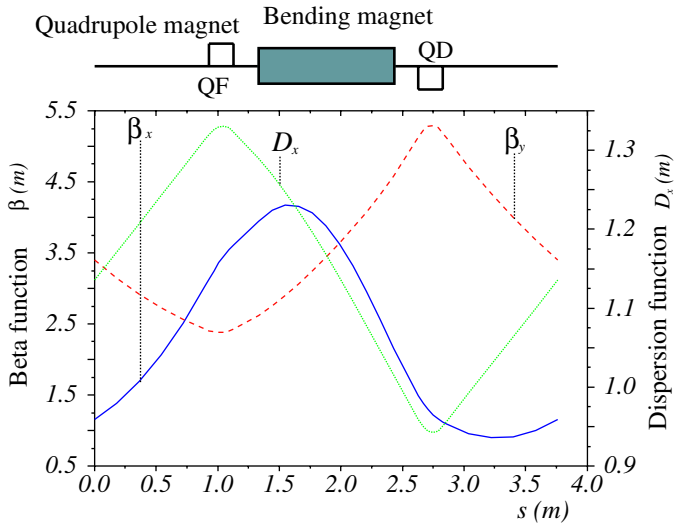

Figure 10. Beta-functions and the dispersion function at the operating point (2.07, 1.07, 0.07) of S-LSR. QF means the quadrupole magnet with a focusing effect in the horizontal direction. QD is the opposite polarity to QF.

3.2. Creation of crystalline beam at S-LSR

3.2.1. Normal operation using only a magnetic field. The lattice of S-LSR has been designed by incorporating the condition mentioned in subsection 3.1. Although the laser cooling is 1D, we make it 3D by using coupling among the three degrees of freedom. Dynamical coupling between the horizontal betatron motion and the synchrotron motion can be created by an rf cavity through dispersion [6]. Coupling between the horizontal and vertical betatron motions is realized by the solenoid of the electron cooler. In order to maximize the coupling effect, the tune values must satisfy the difference resonance conditions;

$$\nu_x - \nu_s = \text{integer}, \qquad \nu_x - \nu_y = \text{integer}. \tag{6}$$

One of the operating points satisfying this condition is $(\nu_x, \nu_y, \nu_s) = (2.07,\ 1.07,\ 0.07)$. At this operating point, the lattice functions take the values as given in figure 10. For a 35 keV $^{24}Mg^{+}$ beam, the required voltage of the rf field is estimated to be 30.7 V and the frequency is 2.32 MHz (for harmonic number 100). The main parameters are listed in table 4. A linear friction force, described as

$$\delta\left(\frac{\Delta p}{p_0}\right) = -f \cdot \left(\frac{\Delta p}{p_0}\right), \tag{7}$$

is applied only in the longitudinal direction as a model of the laser cooling force, where p_0 is the momentum of the reference particle and Δp is the difference in the momentum from p_0. The left-hand side of equation (7) stands for the change in the momentum spread at the cooling section; f is the coefficient of friction. We expect ordered structures, as shown in figure 11, at the final equilibrium state of cooling. 3D crystalline beams, however, cannot be expected due to the shear. Similar results are shown by a multi-particle simulation using a realistic laser cooling model [7, 8].

Table 4. Main parameters of the simulation at the operating point $(\nu_x,\ \nu_y,\ \nu_s) = (2.07,\ 1.07,\ 0.07)$.

Parameter	Value
Ion species	$^{24}Mg^{+}$
Kinetic beam energy	35 keV
Lorentz gamma γ	1.0000016
Transition gamma γ_t	1.757
Harmonic number of the rf cavity	100
Amplitude of the rf field	30.7 V
Axial length of solenoid	0.80 m
Strength of the solenoid field	40 G
Friction coefficient per one turn f_z	0.2

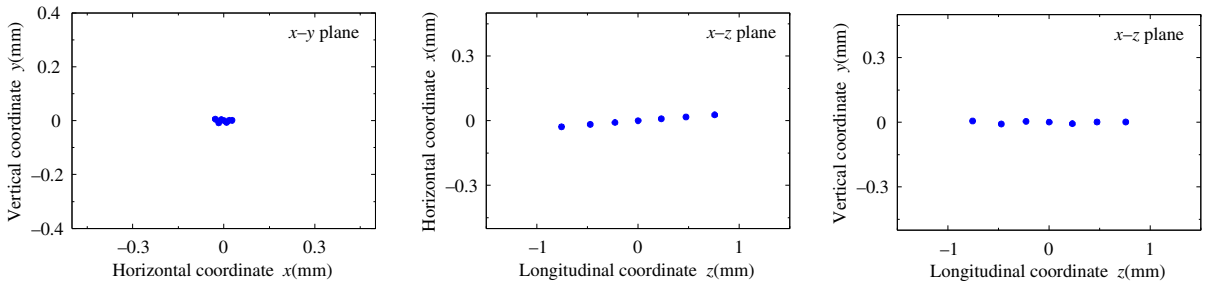

(a) 1D ordering

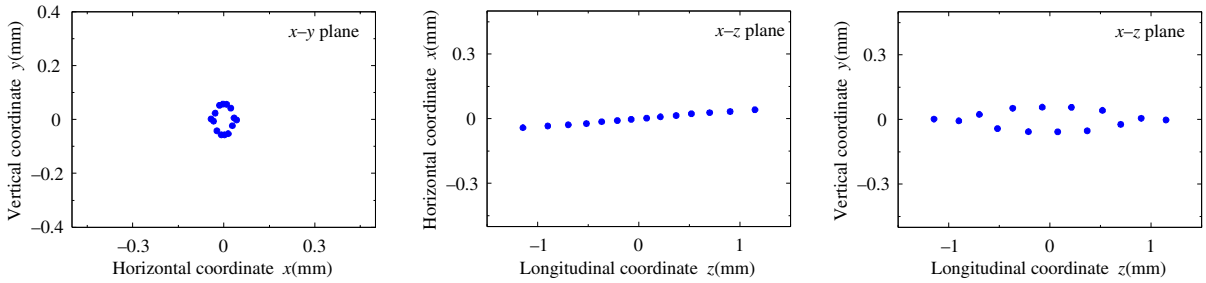

(b) 2D zigzag structure

Figure 11. 1D and 2D crystalline beams expected in S-LSR by a simulation. The cooling force is applied only in the longitudinal direction. The cooling force is extended to a 3D one by applying the resonant coupling method at the operating point (2.07, 1.07, 0.07).

3.2.2. Dispersion-free operation. The idea to overcome shear was first proposed by Pollock [29]. His idea was to use crossed electric and magnetic fields as a deflection field of the circulating beam. Since the scalar potential of the electrostatic field accelerates or decelerates particles at the edges of the deflection element, those particles having the same linear velocity at the straight section can pass through the bending section with the same angular velocity (figure 12). Such a device has been known as a dispersion-free deflector for mass spectrometry [30, 31]. In [32],

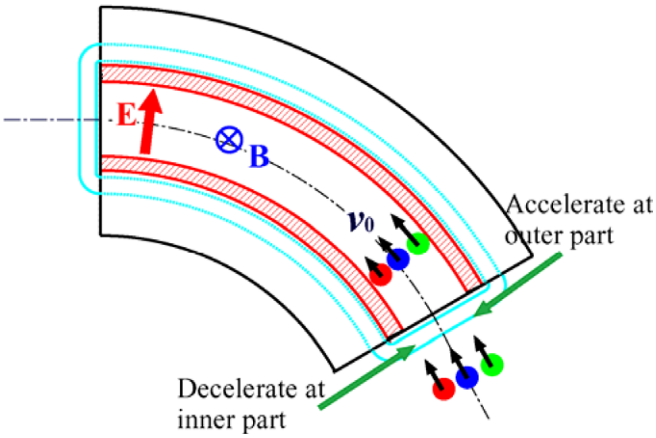

Figure 12. Dispersion-suppressor consisting of crossed electric and magnetic fields. **B** is the magnetic field, **E** is the electric field, $\boldsymbol{v}_0$ is the velocity of the reference particle in the beam. If the relation $(1 + 1/\gamma^2)\,\mathbf{E} = -\boldsymbol{v}_0 \times \mathbf{B}$ is satisfied, the beam is bent without linear dispersion.

based on a Hamiltonian formalism, it is shown that elimination of the dispersion naturally leads to elimination of the shear when the relation $(1 + 1/\gamma^2)\mathbf{E} = -\boldsymbol{v}_0 \times \mathbf{B}$ is satisfied. By detailed beam-dynamics studies concerning dispersion-free storage ring, it is found that a dispersion-free ring satisfying the formation and maintenance conditions for beam crystallization, equations (3) and (4), can be realized at S-LSR with the operating point of $(\nu_x,\ \nu_y,\ \nu_s) = (2.07,\ 2.07,\ 0.07)$ [33]. The beta-functions of this mode are shown in figure 13.

In a dispersion-free ring, the horizontal and longitudinal motions are independent in the range of the linear approximation. Therefore, it is not possible to realize 3D cooling by relying on the dispersion by a normal rf cavity. By introducing a coupling rf cavity [5, 34], coupling between the transverse and longitudinal motions can be obtained without dispersion. For a 35 keV $^{24}Mg^{+}$ beam, the required voltage of the coupling cavity is not very high [35]. Setting the operating point to $(\nu_x,\ \nu_y,\ \nu_s) = (2.07,\ 2.07,\ 0.07)$, the emittance of three directions can be reduced by the resonant coupling method, as shown in figure 14, and 3D crystalline beams, as shown in figure 15, can be expected by avoiding shear [35]. A larger multi-shell crystalline beam, however, cannot be expected due to the blocking of emittance reduction at the resonance crossing during the cooling process.

4. Further approach to a multidimensional crystalline beam

4.1. Tapered cooling

A dispersion-free storage ring is one good approach to producing a multidimensional crystalline beam. The radial focusing of the deflector, however, increases if an electric field is introduced to remove the dispersion. For small storage rings, this effect of radial focusing on the betatron motion is relatively larger, and the betatron tunes are increased. Therefore, in dispersion-free storage rings, it becomes difficult to create multi-shell crystalline beams satisfying the condition of equation (5). In order to satisfy equation (5) at S-LSR with superperiodicity of 6, the betatron tune should be less than 1.5, which is difficult to realize in dispersion-free operation.

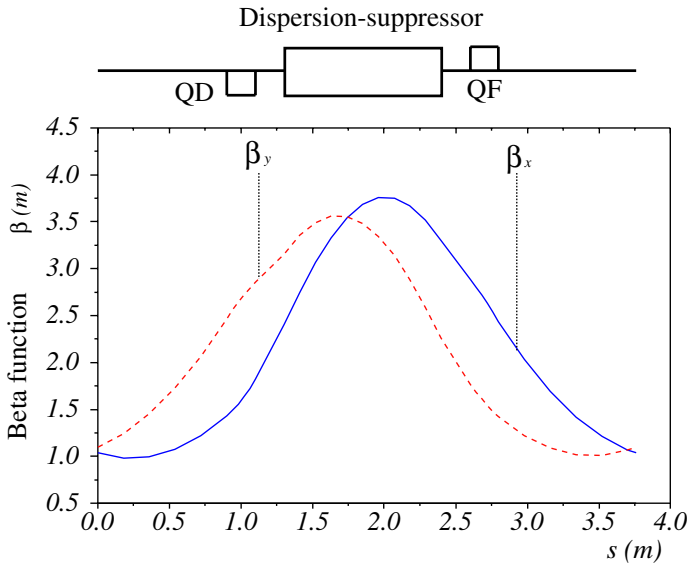

Figure 13. Beta-functions in the dispersion-free operating mode of S-LSR. The betatron tunes are $(\nu_x,\ \nu_y) = (2.07, 2.07)$.

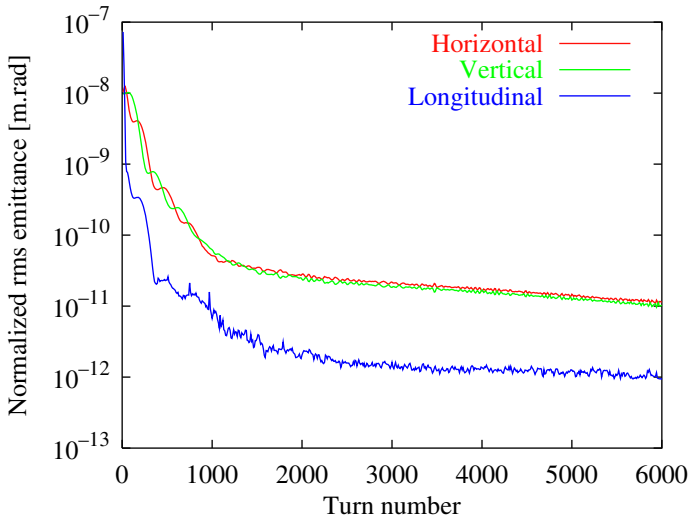

Figure 14. Time evolution of the normalized rms emittance of a 35 keV $^{24}Mg^{+}$ beam cooled with the resonant coupling method by using a coupling cavity in dispersion-free operation. The cooling force is applied only in the longitudinal direction as a linear friction force. Coupling between the longitudinal and horizontal directions is created by the coupling rf cavity. Coupling between the horizontal and vertical directions is created by the solenoidal magnetic field of the electron cooler.

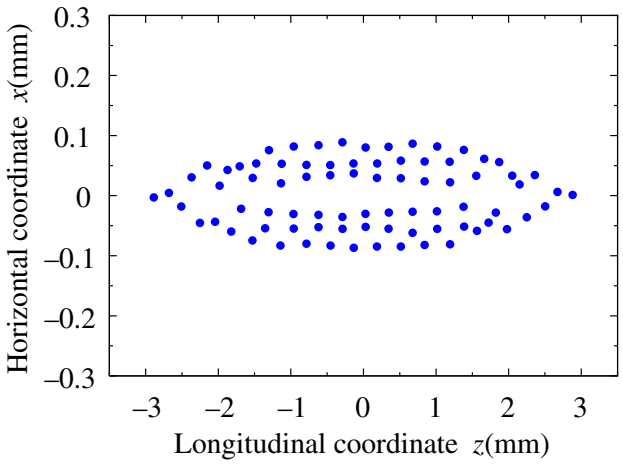

Figure 15. Top view of the crystalline beam generated in the dispersion-free mode of S-LSR by a computer simulation.

Although the effect of shear exists, in the normal operation mode using only a magnetic field, the betatron tune $(\nu_x,\ \nu_y) = (1.44,\ 1.44)$ can be realized.

Another method to overcome shear has been known as 'tapered cooling' [4, 36]. By applying a special longitudinal cooling force depending on the horizontal coordinate x, at the final state of cooling, we can realize the same angular velocity, even in normal storage rings with finite dispersion. The cooling force can be expressed as

$$\delta\left(\frac{\Delta p}{p_0}\right) = -f_z\left(\frac{\Delta p}{p_0} - C_{xs}x\right), \tag{8}$$

where f_z and C_{xs} are positive constant corresponding to the cooling strength and the so-called tapering factor, respectively. At the final equilibrium state of the cooling, the relation $\delta\left(\Delta p/p_0\right) = 0$ is satisfied and the momentum has radial position dependence as,

$$\frac{\Delta p}{p_0} = C_{xs}x. \tag{9}$$

By suitably selecting the value of C_{xs}, the particles have the same angular velocity in the ring. Since the tapered cooling method enables one to stabilize a multidimensional crystalline beam in a normal storage ring with finite dispersion, it is unnecessary to introduce an electric field for dispersion suppression. Therefore, the lower betatron tune value can be kept, with which we can avoid coherent resonances during the cooling process. By application of an ideal tapered cooling force at the operating point of $(\nu_x,\ \nu_y) = (1.44,\ 1.44)$ at S-LSR, multi-shell crystalline beams as shown in figure 16 are expected to be obtained [8].

Although tapered cooling in a normal storage ring is preferable to realize multidimensional crystalline beams, a concrete method to realize tapered cooling has not yet been proposed. The laser cooling force can be somewhat tapered by slightly displacing the laser axis [37, 38]. An accurate adjustment of the magnitude of the tapered factor, however, is extremely difficult with this method. As an alternative idea, a method using potential difference of an electric field has been suggested [39, 40]. For this purpose, we have shown a realistic scheme of tapered cooling using crossed electric and magnetic fields of a Wien filter based on the idea to localize the interaction between the laser and the ion beam only inside the Wien filter [41, 42].

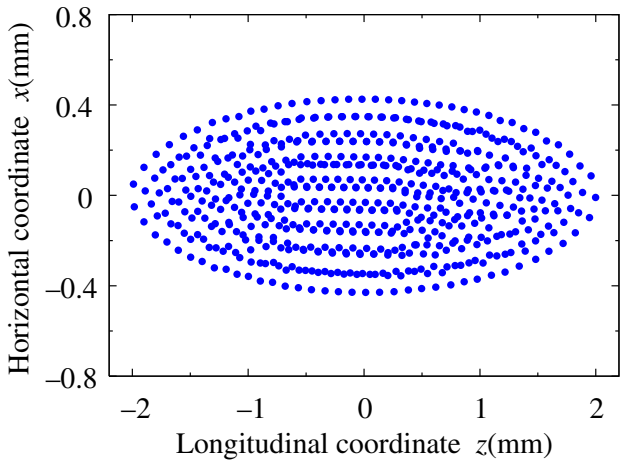

Figure 16. 3D crystalline beam expected by ideal tapered cooling at the operating point, $(\nu_x,\ \nu_Y) = (1.44, 1.44)$ of S-LSR.

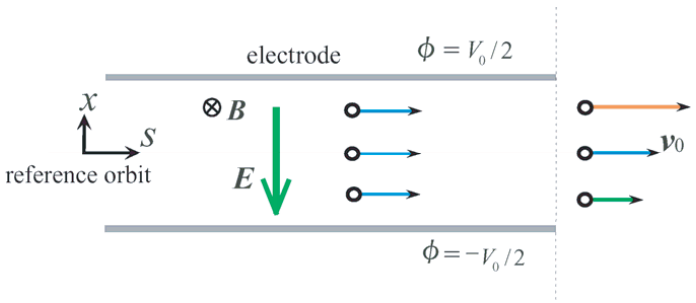

Figure 17. Velocities of the particles at the final equilibrium state of cooling. In the Wien filter, an uniform electric field of strength $|\mathbf{E}| = V_0/d$ is assumed to exist.

4.2. Tapered cooling using a Wien filter

In a Wien filter, the electric field, **E**, and magnetic field, **B**, are superposed so as to not deflect those ions with the design velocity, $\boldsymbol{v}_0$. Then, the following relation is satisfied:

$$\mathbf{E} = -\boldsymbol{v}_0 \times \mathbf{B}. \tag{10}$$

A beam cooling force, such as a laser cooling force, simply equalizes the longitudinal velocity of the particles. If the cooling force acts only in the Wien filter, the longitudinal velocities are equalized in the Wien filter, at the final equilibrium state, as shown in figure 17.

In the Wien filter, a charged particle has a potential energy of ϕ, depending on its horizontal position from the reference orbit, x, as given by

$$\phi = \frac{V_0}{d} \cdot x, \tag{11}$$

where $V_0/2$ and d are the applied voltage to the electrodes and the distance between the electrodes, respectively. Since the electrostatic potential is 0 outside of the Wien filter, the potential energy, ϕ, of the particle is converted to kinetic energy at the exit of the Wien filter. Such kinetic energy depends on the horizontal position where the particle comes out of the Wien filter (figure 17). Therefore, in the final equilibrium state of the cooling, the ions obtain a velocity dependence on the radial position, x. This situation is equivalent to 'tapered cooling'.

In figure 17, the energy of the particle outside the Wien filter has the following value:

$$E = E_0 + \frac{qeV_0}{d} \cdot x, \tag{12}$$

where E_0 is the total energy of the reference particle, $E_0 = m_0\gamma_0 c^2$ (m_0 and γ_0 are the rest mass and the Lorentz factor of the reference particle, respectively), E is the total energy of the particle that has horizontal coordinate x outside of the Wien filter, and q is the charge state of the particle; e is the elementary electric charge. We have assumed that the betatron oscillation is frozen in the crystalline state. The momentum p_0 of the reference particle can be written as $p_0 = \sqrt{E_0^2/c^2 - m_0^2c^2}$. By the same way, the momentum of the particle deviated from the reference orbit can be written as $p = \sqrt{E^2/c^2 - m_0^2c^2} \equiv \sqrt{(E_0 + \Delta E)^2/c^2 - m_0^2c^2}$.

Neglecting the second-order term of ΔE, we obtain

$$\frac{\Delta p}{p_0} \equiv \frac{p - p_0}{p_0} \approx \frac{\Delta E}{\beta_0^2 E_0}, \tag{13}$$

where β_0 is the Lorentz beta of the reference particle; $\beta_0 = v_0/c$. Equation (13) becomes

$$\frac{\Delta p}{p_0} \approx \frac{qeV_0}{\beta_0^2 E_0 d} \cdot x \tag{14}$$

with the use of equation (12).

This equation completely corresponds to tapered cooling, equation (9), with the tapered factor of $qeV_0/\beta_0^2 E_0 d$.

In order to compensate for the difference in the revolution times of the particles in crystalline beams through the whole circumference, the following relations must be satisfied.

$$\frac{\Delta v}{v_0} = \frac{2\pi}{2\pi\rho_0 + N_{\mathrm{sp}}L_{\mathrm{s}}} \cdot x, \tag{15}$$

where ρ_0 and L_{s} are the radius of curvature of the reference orbit at the bending section and the length of the straight section of the ring with N_{sp}-fold symmetry, respectively; v_0 is the velocity of the reference particle, and $v_0 + \Delta v$ is the velocity of the particle, which has horizontal coordinate x. More general derivation of an ideal velocity distribution for complete matching of revolution time considering the space charge effect is given in [43].

The velocity difference generated by the Wien filter can be derived from equation (14) by using the relation

$$\frac{\Delta p}{p_0} \approx \gamma_0^2 \frac{\Delta v}{v_0}, \tag{16}$$

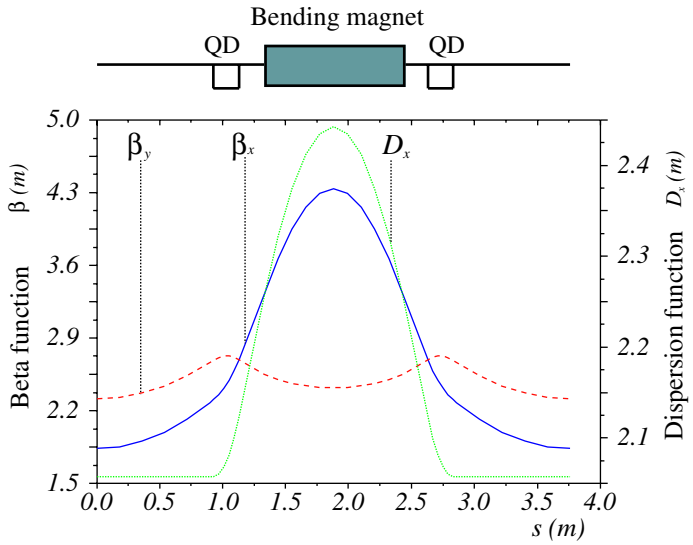

Figure 18. Beta-functions and the dispersion function at the operating point $(\nu_x,\ \nu_y) = (1.44,\ 1.44)$ of S-LSR.

as follows:

$$\frac{\Delta\nu}{\nu_0} \approx \frac{qeV_0}{\beta_0^2\gamma_0^2 E_0 d} \cdot x. \tag{17}$$

By comparing equation (15) with equation (17), the required parameters of the Wien filter are obtained. Substituting the values of S-LSR ($\rho_0 = 1.05\,\mathrm{m}$, $L_\mathrm{s} = 2.66\,m$, $N_\mathrm{sp} = 6$) and the parameters of a 35 keV $^{24}Mg^+$ beam, the strength of the electric field, V_0/d, is calculated to be $19.0\,\mathrm{kV\,m^{-1}}$. The relation between the magnetic and the electric fields of the Wien filter is given by equation (10). Therefore, the magnetic flux density is calculated to be 0.036 T. Both values of the electric and magnetic fields are technically well attainable.

In order to confine the laser cooling process to the inside of the Wien filter, the local overlap between the ion and laser beams using orbit chicane for ion beam has been proposed [41], which, however, is claimed to violate the 'maintenance condition', equation (4), by reducing the superperiodicity to one. A new scheme is proposed to realize such localization of laser cooling by modulating the laser intensity along the direction of the ion passage by using special laser guiding optics [42].

The scheme of the tapered cooling is applied at the operating point $(\nu_x,\ \nu_y) = (1.44,\ 1.44)$ of S-LSR. The lattice functions are as shown in figure 18. At this operating point, it is difficult to apply the resonant coupling method satisfying the difference resonance condition (equation (6)) because of the difficulty of realizing such a high synchrotron tune value as $\nu_s = 0.44$. It should be noted that the tapered cooling automatically realizes cooling of the longitudinal and horizontal degrees of freedom without such resonant coupling [36]. Therefore, by creating only coupling between the horizontal and vertical motions by the solenoid magnetic field, we can develop a 3D cooling force.

5. Conclusion

An approach to an ordered structure of a 7 MeV proton beam has been started experimentally at the ion cooler storage ring, S-LSR. By applying electron-beam cooling reducing the particle number to suppress the IBS effect, the creation of a 1D string has been studied. By the recent measurement reducing the noise level, anomalies in the fractional momentum spread and the Schottky power level for proton numbers less than several thousands have been observed, which might be an indication of 1D ordering of proton beam. In order to clarify the capability of a 1D phase transition of a proton beam with electron beam cooling, theoretical and/or simulation studies on this subject are important as well as our future experimental study further reducing the noise level.

The possibility to obtain multidimensional crystalline beams of $^{24}Mg^{+}$ ions with the kinetic energy of 35 keV by laser cooling has been studied by multi-particle simulations. With the use of laser cooling and resonant coupling method at finite dispersion, it is expected that 1D and 2D crystalline beams can be attained at the operating point $(\nu_x,\ \nu_y) = (2.07,\ 1.07)$ of S-LSR.

There are two methods to reach the 3D crystalline state. The dispersion-free storage rings equipped at S-LSR together with a coupling cavity can generate 3D crystals avoiding the shear. The size of crystal, however, is limited due to the resonance crossing because of the betatron tune at $(\nu_x,\ \nu_y) = (2.07,\ 2.07)$.

Tapered cooling can overcome the shear, keeping lower betatron tune with finite dispersion. We have proposed a new practical method to realize the tapered cooling confining the laser cooling inside a Wien filter, which is shown to be equivalent to the tapered cooling. When the Wien filter is introduced to S-LSR at the operating point $(\nu_x,\ \nu_y) = (1.44,\ 1.44)$, larger multi-layer 3D crystalline beams with higher line density are expected.

Acknowledgments

The study presented here has been supported by Advanced Compact Accelerator Development project by MEXT of Japanese Government. Support from the 21st Century COE at Kyoto University–Diversity and Universality in Physics is also greatly appreciated.

References

[1] Parkhomchuk V 1984 Physics of fast electron cooling *Proc. Workshop on Electron Cooling and Related Applications (ECOOL84) (KfK Report No 3846)* ed H Poth (KfK, Karlsruhe) pp 71–83
[2] Steck M, Beckert K, Eickhoff H, Franzke B, Nolden F, Reich H, Schlitt B and Winkler T 1996 *Phys. Rev. Lett.* **77** 3803
[3] Danared H, Källberg A, Rensfelt K-G and Simonsson A 2002 *Phys. Rev. Lett.* **88** 174801
[4] Wei J, Okamoto H and Sessler A M 1998 *Phys. Rev. Lett.* **80** 2606
[5] Okamoto H, Sessler A M and Möhl D 1994 *Phys. Rev. Lett.* **72** 3977
[6] Okamoto H 1994 *Phys. Rev.* E **50** 4982
[7] Yuri Y and Okamoto H 2004 *Phys. Rev. Lett.* **93** 204801
[8] Yuri Y and Okamoto H 2005 *Phys. Rev. ST Accel. Beams* **8** 114201
[9] Schätz T, Schramm U and Habs D 2001 Crystalline ion beams, *Nature (London)* **412** 717–20
[10] Wei J, Li X-P and Sessler A M 1994 *Phys. Rev. Lett.* **73** 3089
[11] Noda A 2004 *Nucl. Instrum. Methods* A **532** 150
[12] Steck M 1997 *Nucl. Phys.* A **626** 473

[13] Hasse R W 2004 *Nucl. Instrum. Methods* A **532** 382
[14] Meshkov I and Sidorin A 2004 *Nucl. Instrum. Methods* A **532** 474
[15] Okamoto H, Okabe K, Yuri Y, Möhl D and Sessler A M 2004 *Phys. Rev.* E **69** 066504
[16] Steck M, Beller P, Beckert K, Franzke B and Nolden F 2004 *Nucl. Instrum. Methods* A **532** 357
[17] Dietrich J, Meshkov I, Sidorin A, Smirnov A and Stein J 2005 *Proc. Int. Workshop on Beam Cooling and Related Topics, COOL05* ed S Nagaitsev and R J Pasquinelli (Galena, IL) pp 154–58
[18] Dikansky N S *et al* 1988 *INP Preprint* 88–61
[19] Fadil H, Grieser M, Noda A, Noda K, Shirai T and Syresin E 2004 *Nucl. Instrum. Methods* A **532** 446
[20] Ellert Ch *et al* 1992 *Nucl. Instrum. Methods* A **314** 399
[21] Smirnov A, Noda A, Shirai T and Ikegami M 2006 Crystalline beams at S-LSR *Beam Science and Technology* vol 10, ed M Ikegami (Uji: ICR Kyoto University) pp 6–12
[22] Online at http://lepta.jinr.ru/betacool.htm
[23] Yonehara H, Tokuda N, Yoshizawa M and Hattori T 1983 *Equipments For Momentum Cooling At Tarn* Report No. *INS-NUMA*-**49** (Tanashi: INS University of Tokyo)
[24] Fujimoto S, Shirai T, Tongu H, Souda H, Noda A, Takeuchi T and Noda K 2005 *Proc. of 36th ICFA Advanced Beam Dynamics Worcshop, NANOBEAM 2005* ed Y Honda, T Tauchi, J Urakawa, Y Iwashita and A Noda (Uji: ICR Kyoto University) pp 441–3
[25] Rahman A and Schiffer J P 1986 *Phys. Rev. Lett*. **57** 1133
[26] Hasse R W and Schiffer J P 1990 *Ann. Phys., NY* **203** 419
[27] Li X-P, Enokizono H, Okamoto H, Yuri Y, Sessler A M and Wei J 2006 *Phys. Rev. ST Accel. Beams* **9** 034201
[28] Okabe K and Okamoto H 2003 *Japan. J. Appl. Phys*. **42** 4584
[29] Pollock R E 1991 *Z. Phys. A: Hadrons and Nuclei* **341** 95
[30] Henneberg W 1934 *Ann. Phys., Lpz.* **19** 335
[31] Millett W E 1948 *Phys. Rev.* **74** 1058
[32] Ikegami M, Noda A, Tanabe M, Grieser M and Okamoto H 2004 *Phys. Rev. ST Accel. Beams* **7** 120101
[33] Ikegami M, Iwashita Y, Souda H, Tanabe M and Noda A 2005 *Phys. Rev. ST Accel. Beams* **8** 124001
[34] Kihara T, Okamoto H, Iwashita Y, Oide K, Lamanna G and Wei J 1999 *Phys. Rev.* E **59** 3594
[35] Ikegam M, Okamoto H and Yuri Y, in preparation
[36] Okamoto H and Wei J 1998 *Phys. Rev.* E **58** 3817
[37] Lauer I, Eisenbarth U, Grieser M, Grimm R, Lenisa P, Luger V, Schätz T, Schramm U, Schwalm D and Weidemüller M 1998 *Phys. Rev. Lett*. **81** 2052
[38] Kjærgaard N and Drewsen M 1999 *Phys. Lett.* A **260** 507
[39] Meshkov I N 1974 *Doctoral Thesis* Budker INP, Novosibirsk
[40] Madsen N 1998 *PhD Thesis* University of Aarhus
[41] Noda A and Grieser M 2005 *Beam Science and Technology* vol 9, ed T Shirai (Uji: ICR Kyoto University) p 12
[42] Noda A, Ikegami M, Sakabe S and Aruga T 2006 *Beam Science and Technology* vol 10, ed M Ikegami (Uji: ICR Kyoto University) p 39
[43] Okamoto H 2002 *Phys. Plasmas* **9** 322